



Genetic Determinants Enabling Medium-Dependent Adaptation to Nafcillin in Methicillin-Resistant *Staphylococcus aureus*

Michael J. Salazar,^a  Henrique Machado,^a Nicholas A. Dillon,^b Hannah Tsunemoto,^c Richard Szubin,^a Samira Daresh,^b Joseph Pogliano,^{b,f} George Sakoulas,^b Bernhard O. Palsson,^{a,b,d}  Victor Nizet,^{b,d}  Adam M. Feist^{a,e}

^aDepartment of Bioengineering, University of California San Diego, La Jolla, California, USA

^bCollaborative to Halt Antibiotic-Resistant Microbes, Department of Pediatrics, University of California San Diego, La Jolla, California, USA

^cDepartment of Biology, University of California San Diego, La Jolla, California, USA

^dSkaggs School of Pharmacy and Pharmaceutical Sciences, University of California San Diego, La Jolla, California, USA

^eNovo Nordisk Foundation Center for Biosustainability, Technical University of Denmark, Lyngby, Denmark

^fDivision of Biological Sciences, University of California San Diego, La Jolla, California, USA

Michael J. Salazar and Henrique Machado contributed equally to this work. Author order was determined by seniority in the project.

ABSTRACT Antimicrobial susceptibility testing standards driving clinical decision-making have centered around the use of cation-adjusted Mueller-Hinton broth (CA-MHB) as the medium with the notion of supporting bacterial growth, without consideration of recapitulating the *in vivo* environment. However, it is increasingly recognized that various medium conditions have tremendous influence on antimicrobial activity, which in turn may have major implications on the ability of *in vitro* susceptibility assays to predict antibiotic activity *in vivo*. To elucidate differential growth optimization and antibiotic resistance mechanisms, adaptive laboratory evolution was performed in the presence or absence of the antibiotic nafcillin with methicillin-resistant *Staphylococcus aureus* (MRSA) TCH1516 in either (i) CA-MHB, a traditional bacteriological nutritionally rich medium, or (ii) Roswell Park Memorial Institute (RPMI), a medium more reflective of the *in vivo* host environment. Medium adaptation analysis showed an increase in growth rate in RPMI, but not CA-MHB, with mutations in *apt*, adenine phosphoribosyltransferase, and the manganese transporter subunit, *mntA*, occurring reproducibly in parallel replicate evolutions. The medium-adapted strains showed no virulence attenuation. Continuous exposure of medium-adapted strains to increasing concentrations of nafcillin led to medium-specific evolutionary strategies. Key reproducibly occurring mutations were specific for nafcillin adaptation in each medium type and did not confer resistance in the other medium environment. Only the *varST* operon, a regulator of membrane- and cell wall-related genes, showed mutations in both CA-MHB- and RPMI-evolved strains. Collectively, these results demonstrate the medium-specific genetic adaptive responses of MRSA and establish adaptive laboratory evolution as a platform to study clinically relevant resistance mechanisms.

IMPORTANCE The ability of pathogens such as *Staphylococcus aureus* to evolve resistance to antibiotics used in the treatment of infections has been an important concern in the last decades. Resistant acquisition usually translates into treatment failure and puts patients at risk of unfavorable outcomes. Furthermore, the laboratory testing of antibiotic resistance does not account for the different environment the bacteria experiences within the human body, leading to results that do not translate into the clinic. In this study, we forced methicillin-resistant *S. aureus* to develop nafcillin resistance in two different environments, a laboratory environment and a physiologically more relevant environment. This allowed us to identify genetic

Citation Salazar MJ, Machado H, Dillon NA, Tsunemoto H, Szubin R, Daresh S, Pogliano J, Sakoulas G, Palsson BO, Nizet V, Feist AM. 2020. Genetic determinants enabling medium-dependent adaptation to nafcillin in methicillin-resistant *Staphylococcus aureus*. *mSystems* 5:e00828-19. <https://doi.org/10.1128/mSystems.00828-19>.

Editor Christopher W. Marshall, Marquette University

Copyright © 2020 Salazar et al. This is an open-access article distributed under the terms of the [Creative Commons Attribution 4.0 International license](https://creativecommons.org/licenses/by/4.0/).

Address correspondence to Adam M. Feist, afeist@ucsd.edu.

 Environment dictates the evolutionary strategy of *S. aureus* towards antibiotic resistance.

Received 12 December 2019

Accepted 11 March 2020

Published 31 March 2020

changes that led to nafcillin resistance under both conditions. We concluded that not only does the environment dictate the evolutionary strategy of *S. aureus* to nafcillin but also that the evolutionary strategy is specific to that given environment.

KEYWORDS *Staphylococcus aureus*, antibiotic resistance, nafcillin, USA300, adaptive laboratory evolution, drug resistance mechanisms

Staphylococcus aureus is a commensal Gram-positive bacteria that colonizes human skin, as well as nasal and respiratory tracts. Upon breaching skin or mucosal barriers, *S. aureus* can cause infections of skin, blood, and tissues (1). Although historically associated with hospital and health care infections, community-acquired methicillin-resistant *S. aureus* (CA-MRSA) infections are now widespread globally (2), of which USA300 is the most common clonal lineage in North America (3). MRSA TCH1516 is a well-studied representative USA300 strain isolated from an adolescent at the Texas Children's Hospital in Houston with severe sepsis (4).

In vitro methods for evaluating antibiotic activity against bacterial pathogens were developed and standardized in 1961 as a "one size fits all" screen (5). This method has been paramount in antibiotic research, but translation to *in vivo* efficacy has been increasingly questioned (6, 7). Determination of the MIC for potential drugs has also varied considerably between "standard" testing media from different manufacturers (8) and with additionally supplemented cations (9). Differential susceptibility is even more pronounced between traditional testing media and more physiologically relevant medium conditions (i.e., taking factors such as supplemented cations, interaction with host factors, and nutrient availability into consideration) (10–12). In this study, differential antibiotic response was examined between standard bacteriological testing medium cation-adjusted Mueller-Hinton broth (CA-MHB) and Roswell Park Memorial Institute (RPMI) medium, a medium used in cell and tissue culture for mammalian cells, supplemented with 10% Luria-Delbruck (LB) (RPMI + 10%LB).

Despite the implications of medium-specific susceptibility of important pathogens, little work has been done to understand any medium-specific differential genetic response to tolerance under an antibiotic stress. Adaptive laboratory evolution (ALE) is an appropriate tool that can be utilized to meet this challenge and study the adaptive capabilities of microorganisms *in vitro*, as mutants that have differential resistance properties can be identified in a straightforward manner. ALE has been applied to study the adaptive response to a number of external stressors such as temperature (13, 14) or antibiotics (15–17). Specifically relevant to *S. aureus*, previous studies have utilized ALE to study the adaptive capabilities to various antibiotics (18–22). These studies have enabled an assessment of current and potential treatment strategies via identification of mutational targets and associated phenotypic changes that confer resistance to antibiotics of interests. Antistaphylococcal beta-lactams (e.g., nafcillin, oxacillin, flu-cloxacillin, cloxacillin) are the treatment of choice against serious methicillin-susceptible *S. aureus* (MSSA) infections (23, 24). A representative of this class, nafcillin, has been identified as one of the antibiotics with medium-dependent efficacies (11), making it an ideal candidate for this study. The Clinical and Laboratory Standards Institute (CLSI) breakpoint for nafcillin in CA-MHB is greater than or equal to 4 $\mu\text{g}/\text{ml}$, and susceptible is less than or equal to 2 $\mu\text{g}/\text{ml}$.

In this work, ALE was applied to uncover medium-specific mechanisms of resistance to nafcillin in a controlled setting. First, ALE was implemented to adapt *S. aureus* TCH1516 to both medium conditions (CA-MHB and RPMI + 10%LB), in order to optimize cellular performance and establish a suitable baseline with which to compare any further evolutionary work. Second, ALE was harnessed to study nafcillin resistance of such medium-adapted strains in order to gain insights into the genetic basis for adaptation in differing medium conditions. Finally, resistant strains were assessed for growth rate, effective nafcillin resistance, and virulence capabilities, so phenotypic trade-offs could be identified.

RESULTS

Laboratory evolution for adaptation to medium environments. *S. aureus* TCH1516 was forced to evolve under two medium conditions to understand how it adapts under growth rate selection to different nutritional environments. The two chosen medium types were CA-MHB and RPMI + 10%LB (referred to as RPMI+), since differential susceptibility to nafcillin was observed across both conditions (see Table S1 in the supplemental material) (11). Five independent populations of *S. aureus* TCH1516 were forced to evolve on CA-MHB, while eight independent populations were forced to evolve on RPMI+ for an average of 108 and 100 batch flask transfers, respectively (Table S2). Flask transfers were performed when an optical density at 600 nm (OD_{600}) of 0.3 ± 0.02 or 0.434 g (dry weight [DW])/liter was achieved to prevent the cells from entering stationary phase, thus selecting for advantages in growth rate. Although no growth rate improvements were observed for evolutions performed in CA-MHB, population growth rates for *S. aureus* on RPMI+ increased from a starting wild-type growth rate of $0.75 \pm 0.1 \text{ h}^{-1}$ to $1.1 \pm 0.1 \text{ h}^{-1}$, an ~ 1.5 -fold increase, during a range of 4.52×10^{12} to 5.26×10^{12} cumulative cell cycle divisions (CCD) (Fig. 1A and B). CCD has previously been shown to effectively represent the time scale for ALEs in contrast to elapsed time or generations (25). It should be noted that the overall growth rate of the population at the end of the evolution on RPMI+ ($1.06 \pm 0.10 \text{ h}^{-1}$) was similar to that of the starting growth rate on CA-MHB ($1.12 \pm 0.083 \text{ h}^{-1}$) (Table S2). Clonal isolates were selected from each of the final flasks of the independently evolved populations of the medium adaptation ALEs (i.e., endpoint clones) to RPMI+ (eight clones) and CA-MHB (five clones) in order to explore the phenotypes from the isolated evolved genotypes. Growth rates were measured for each of the endpoint clones, and there was concordance between the values observed for the populations at the end of the evolutions. The increase in growth rate of *S. aureus* TCH1516 through adaptation to RPMI+, but not to CA-MHB, was confirmed on the clonal level. Similar work has been performed forcing *S. aureus* to evolve in various medium conditions, although growth rates were not reported (26, 27). The identical growth rate between the two conditions evaluated here indicates an apparent maximum achievable growth rate for strain TCH1516 in a batch growth rich medium environment, given the stated evolution times. Following medium adaptation, the medium-adapted strains were evaluated for their virulence capabilities and sequenced to explore the genetic mechanisms behind observed fitness improvements.

Medium-adapted strain virulence in a murine model of pneumonia. Continued passaging of pathogenic strains of bacteria *in vitro* can lead to attenuation, yielding derived laboratory strains that are disparate to those seen within patients (28). As multiple dedicated pathways are essential for virulence within a host, it is often the case that laboratory-evolved strains become nonpathogenic, due to the disruption of those pathways, leading to attenuation, therefore decreasing their clinical relevance. A murine pneumonia infection model was used to examine the virulence of medium-adapted strains in comparison to the pathogenic TCH1516 parental lineage. This model utilizes an intratracheal injection to establish a bacterial pneumonia and has been previously used to assess lung bacterial burdens (29). Surprisingly, despite RPMI+ serving as a better mimic for physiological conditions, strains that were adapted to RPMI+ did not have a virulence advantage within the host compared to those adapted to the standard laboratory growth medium (Fig. 1C). It was determined that medium-adapted strains maintain their pathogenicity and had no gross virulence defects in comparison with the TCH1516 parental lineage, indicating that these strains were not attenuated.

Mutation analysis of whole-genome resequencing for medium adaptation. Whole-genome sequencing was performed on evolved populations and selected clones from the ALE experiments on the two selected medium types to explore whether mutations could be linked to the observed fitness improvements. Sequences were analyzed to determine mutations from the multiple replicates under each con-

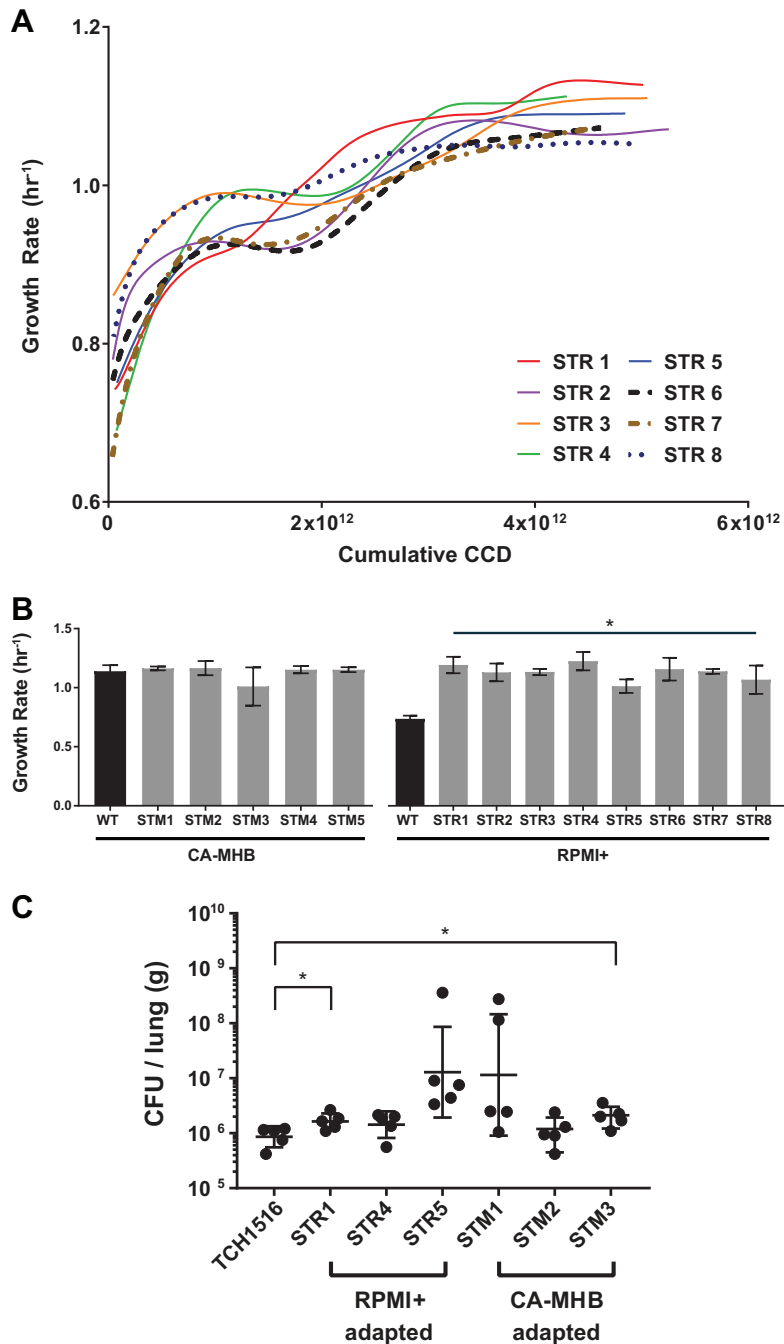


FIG 1 Medium adaptation of *S. aureus* TCH1516. (A) Fitness trajectories depicting growth rate increase throughout the course of the medium adaptation ALE in RPMI+. Strains STR 1, 4, and 5 served as progenitors for the medium-adapted starting points in the tolerance evolution. (B) Clonal growth rates for single clones isolated by streaking endpoint populations. Measurements were determined from biological duplicates and an average of two consecutive flasks. STR strains are *S. aureus* RPMI+-adapted strains. STM strains are *S. aureus* CA-MHB-adapted strains. Values that are significantly different ($P < 0.0001$) from the value for the wild type (WT) by two-way ANOVA are indicated by a bar and asterisk. (C) ALE-derived strains maintain parental lineage virulence in a murine pneumonia model of infection. Values that are significantly different ($P < 0.05$) by *t* test with Welch's correction are indicated by a bar and asterisk.

dition (30, 31). For the CA-MHB condition, only endpoint clones were sequenced given the lack of an apparent fitness change during the course of the evolution, and a total of three unique mutations were found across all five replicates (two clones had no mutations detected [Table S3]). For the RPMI+ condition, there were 261 unique

TABLE 1 Key reproducibly occurring mutations detected in the final populations and clones of *S. aureus* TCH1516 after adaptive laboratory evolution in RPMI+

Gene ^a	Specific function	Mutation type ^b	Protein and nucleotide change ^c	Strain(s) ^d
<i>apt</i>	Adenine phosphoribosyl transferase	SNP	D119E (GAT→GAA)	8
		SNP	H104Y (CAC→TAC)	1
		SNP	P76S (CCT→TCT)	6p
		SNP	G73D (GGC→GAC)	4
		SNP	A67V (GCT→GTT)	2p, 6, 7
		SNP	A67T (GCT→ACT)	5
		SNP	V66L (GTA→CTA)	1p
		SNP	V41L (GTA→TTA)	2
<i>mntA</i> (<i>znuC_1</i>)	Manganese ABC transporter	SNP	L11I (TTA→ATA)	4
		SNP	L2I (TTA→ATA)	2p
		SNP	M1M (TTG→ATG)†	3, 5, 6p, 7
<i>mntA</i> , <i>mntR</i> (<i>znuC_1</i> , <i>ideR</i>)	Manganese ABC transporter/Mn-dependent transcriptional regulator MntR	SNP	A→G, intergenic (−1/−121)	4
		SNP	C→T, intergenic (−2/−120)	2p
		INS	(GTTTAGGCTAACCTAATTAA)1→2, intergenic (−43/−79)	3, 5, 6p, 7
<i>stk1</i> (<i>prkC</i>)	Serine/threonine-protein kinase	SNP	A124P (GCG→CCG)	4
		SNP	V470D (GTT→GAT)	1
<i>cspA_2</i>	Cold shock protein CspA	SNP	A60V (GCT→GTT)	2
		DEL	Δ1 bp, coding (34/201 nt)	4
<i>dynA</i> (RS07370)	Bacterial dynamin-like protein	SNP	Q1098E (CAA→GAA)	2
		SNP	S618T (TCT→ACT)	6
<i>recJ</i>	Single-stranded-DNA-specific exonuclease RecJ	SNP	S757S (TCG→TCT)	3
		SNP	A348V (GCA→GTA)	8
<i>lyrA</i>	Lysostaphin resistance protein A	SNP	L48L (CTA→CTT)	1
		DEL	Δ1 bp, coding (1210/1260 nt)	5
		SUB	2 bp→AT, coding (1216 – 1217/1260 nt)	5

^aThe gene locus tag corresponds to USA300HOU_RSXXXXX. The gene nomenclature provided by prokka annotation, reflected in the mutation analysis, is shown in the parentheses.

^bSNP, single nucleotide polymorphism; INS, insertion; DEL, deletion; SUB, substitution.

^cnt, nucleotide; †, mutation led to formation of a start codon.

^dp denotes population.

mutations across all of the intermediate and endpoint populations and clones selected during the experiment, with the clones having between 4 and 12 mutations each (Table S4). To focus the analysis, mutations were labeled as “key mutations” if a gene or genetic region contained multiple unique mutations across replicates or if an identical mutation appeared across independent ALE replicates. For RPMI+, there were eight genes or genetic regions that met these criteria, with three having greater than two instances. A summary of the RPMI+ medium adaptive mutations is shown in Table 1. For CA-MHB, there was no gene which shared mutations across two of the endpoint clones.

In RPMI+ medium conditions, the most prevalent gene that mutated was *apt*, with all independent replicates containing at least one mutation in this gene, which remained present in the majority of endpoint clones (Table 1). The *apt* gene encodes an adenine phosphoribosyltransferase which enables nucleotide salvage reactions converting adenine to AMP (32). Mutations in this gene have also been discovered after *in vitro* passaging of *S. aureus* after exposure to increasing concentrations of vancomycin (18). Constructed *apt* deletion mutants experienced significant reduction in extracellular DNA (eDNA) release, a major constituent for biofilm stability and formation, low production of extra polymeric substances (33, 34), as well as increased resistance to Congo red (35).

An additional highly mutated region for growth rate optimization on RPMI+ was the *mntA* gene and its intergenic region upstream of both *mntA* and its regulator *mntR*. The *mntA* gene encodes a manganese permease subunit of an ATP binding transporter, while *mntR* encodes a metal-dependent transcriptional regulator (36). An identical mutation was identified in the start codon of *mntA* across three independent ALEs, modifying the initiation site from a suboptimal form (UUG) to AUG, which is the optimal start codon in prokaryotes (37, 38). Mutations in the intergenic region include two single nucleotide polymorphisms (SNPs) occurring 1 and 2 nucleotides upstream of *mntA*, likely affecting its promoter. The other intergenic change was an insertion of a 20-nucleotide sequence, 43 bp upstream of *mntA*. Acquisition of manganese is important for cell survival and replication of pathogens and is crucial for cell detoxification of reactive oxygen species (39). Inactivation of the MntABC transporter complex in another USA300 strain has been shown to attenuate virulence in *in vivo* mouse models (40). Manganese acquisition appears to be particularly relevant in endovascular infections. Disruption of *mntA*, *mntH*, *mntR*, or both *mntA* and *mntH* also significantly reduces intracellular survival in human endothelial cells. Bioavailable Mn is utilized by *S. aureus* to detoxify reactive oxygen species and protect against neutrophil killing, enhancing the ability to cause endocardial infections (41, 42).

Additional key mutations were identified in the RPMI+ growth rate adaptation: mutations in two genes encoding regulatory proteins, *cspA* and *stk1*, and in the *dynA*, *recJ*, and *lyrA* genes, encoding a GTPase, an exonuclease, and a protease, respectively (Table 1; see also Text S1 in the supplemental material).

The medium-adapted strains were subsequently used to understand *S. aureus*' tolerization to nafcillin, with the goal of identifying the genetic basis of this process in the different medium environments.

Laboratory evolution for adaptation to nafcillin tolerance. A tolerance adaptive laboratory evolution (TALE) experiment was implemented to force medium-adapted strains of *S. aureus* TCH1516 to develop resistance to the β -lactam antibiotic nafcillin and identify mutations enabling an elevated growth rate under increasing antibiotic stress concentrations in both CA-MHB and RPMI+ medium environments. The *S. aureus* strains selected as starting strains of the TALE experiments consisted of the respective medium-adapted strains, denoted STM (CA-MHB) and STR (RPMI+). The starting strains for the TALE experiments were medium-adapted strains with distinct genotypes (Table 2).

TALE proved to be effective in developing strains with increased resistance to nafcillin in both RPMI+ and CA-MHB. Three medium-adapted starting strains per medium type (STM 1, 2, and 3 and STR 1, 4, and 5) were forced to evolve in duplicate or triplicate to generate a total of 14 independent evolutions (Table 2). Figure 2A details a typical TALE trajectory of the growth rate and the continuously increasing concentration of nafcillin in RPMI+ (Fig. S1 shows a CA-MHB nafcillin typical TALE trajectory). Over the course of evolution, *S. aureus* populations underwent an average of 3.93×10^{12} CCD and 72 flasks for CA-MHB and 13.81×10^{12} CCs and 175 flasks for RPMI+. Evolutions on RPMI+ were noticeably longer (Table 2) due to the differential susceptibility of *S. aureus* TCH1516 to nafcillin in the two medium conditions (11) (Table S1). The MIC on RPMI+ was ~ 100 -fold less compared to the MIC on CA-MHB for the respective starting strains (Table S5). The initial starting concentrations of nafcillin for the TALEs were therefore adjusted to ensure cell viability. Concentrations of nafcillin reached as high as $600 \times \text{MIC}_{90}$ on RPMI+ and $8 \times \text{MIC}_{90}$ on CA-MHB (Table 2) compared to the wild type on their respective medium.

Endpoint clonal isolates from each of the independent TALE replicates were selected to assess and confirm the increased nafcillin resistance phenotype. As expected, nafcillin resistance for the evolved clones was increased. However, the increase in tolerance observed for isolated clones did not quantitatively match the values tolerated by the TALE populations from which they were isolated (Fig. 2B). In RPMI+, an MIC_{90} ranging from 10 to 20 $\mu\text{g/ml}$ was achieved for isolated clones compared to a range of

TABLE 2 Tolerance phenotypes for *S. aureus* USA300_TCH1516 and medium-adapted evolved populations on CA-MHB and RPMI+^a

Ancestor strain and strain	ALE no.	Initial growth rate (h ⁻¹)	Starting nafcillin concn (μg/ml)	Final growth rate (h ⁻¹)	Final nafcillin concn (μg/ml)	No. of flasks	CCD × 10 ¹²
RPMI+ TALE (SNFR)							
STR 1	7	1.17 ± 0.02	0.013	0.83 ± 0.12	65.52	184	15.2
	9	1.20 ± 0.03	0.013	0.83 ± 0.08	50.4	174	13.4
STR 4	13	1.23 ± 0.08	0.013	0.85 ± 0.09	83.16	191	14.5
	15	1.17 ± 0.08	0.013	0.83 ± 0.06	57.96	177	14.2
	17	1.04 ± 0.07	0.013	0.74 ± 0.11	65.52	172	13.6
STR 5	19	1.11 ± 0.1	0.013	0.87 ± 0.14	52.92	166	12.8
	21*	1.19 ± 0.04	0.013	0.99 ± 0.08	4.32	117	8.5
	23	1.22 ± 0.08	0.013	0.89 ± 0.14	57.96	171	13.6
CA-MHB TALE (SNFM)							
STM 1	7	0.79 ± 0.07	0.5	0.77 ± 0.17	61.2	72	3.94
	11	0.90 ± 0.12	0.5	0.87 ± 0.07	80.33	75	4.08
STM 2	13	0.94 ± 0.11	0.5	0.70 ± 0.03	61.2	68	3.75
	15	0.87 ± 0.14	0.5	0.76 ± 0.13	61.2	70	3.81
STM 3	19	0.97 ± 0.16	0.5	0.88 ± 0.08	61.2	74	3.95
	23	0.93 ± 0.11	0.5	0.93 ± 0.06	61.2	74	4.16

^aPopulation growth rates for independent replicates were calculated by averaging the initial and final three flasks of the medium adaptation ALEs. An asterisk indicates premature end to experiment due to technical errors.

45 to 83 μg/ml observed in population endpoints. The same phenomenon was observed in a smaller degree for isolated clones from the TALE in CA-MHB. The MIC₉₀ of nafcillin for CA-MHB TALE isolates ranged between 31.3 and 50 μg/ml compared to 61 to 87 μg/ml measured for TALE final evolved populations (Fig. 2B and Table 2). This can likely be attributed to population dynamics, kin selection (43), “bacterial cheating,” where overproduction of degradative enzymes can inactivate antibiotic molecules (44), or simply due to a difference in culturing methods under which the clonal MICs were determined compared to the culturing conditions during the TALE experiment (see Materials and Methods).

To assess phenotypic trade-offs in the evolved strains, endpoint clonal growth rates were measured in their evolutionary medium as well as the alternate medium type utilized in this study (i.e., a medium swap) under no nafcillin stress. Characterizations were performed with both medium- and nafcillin-adapted clones. As shown above (Fig. 1B), RPMI+ medium-adapted strains (STR) saw a 52% increase in growth rate compared to the wild-type *S. aureus* TCH1516 (two-way analysis of variance [ANOVA], $P < 0.0001$) (Table S6). Medium adaptation to CA-MHB (STM) did not confer a fitness advantage in RPMI+ (two-way ANOVA, $P = 0.8745$). Strains with a higher resistance to nafcillin in RPMI+ (SNFR) resulted in a fitness tradeoff compared to medium-adapted strains in the same medium (STR) with an overall 11% decrease in growth rate (two-way ANOVA, $P = 0.0054$) (Fig. 3A and Table S6). For the medium swap conditions, there was an unexpected growth rate increase of 29% for strains evolved for resistance to nafcillin in CA-MHB (SNFM) when grown in RPMI+ compared to the progenitor strains that were adapted to CA-MHB (STM) (two-way ANOVA, $P < 0.0001$) (Fig. 3A and Table S6). There were no significant changes in growth rates observed across any of the strains analyzed in CA-MHB medium (Table S6).

Mutational analysis for tolerance evolutions. Whole-genome sequencing was performed on evolved populations and selected clones from TALEs on both medium types to determine shared or unique mutational mechanisms of nafcillin resistance phenotypes. Key mutations were again identified in a similar manner to those from the

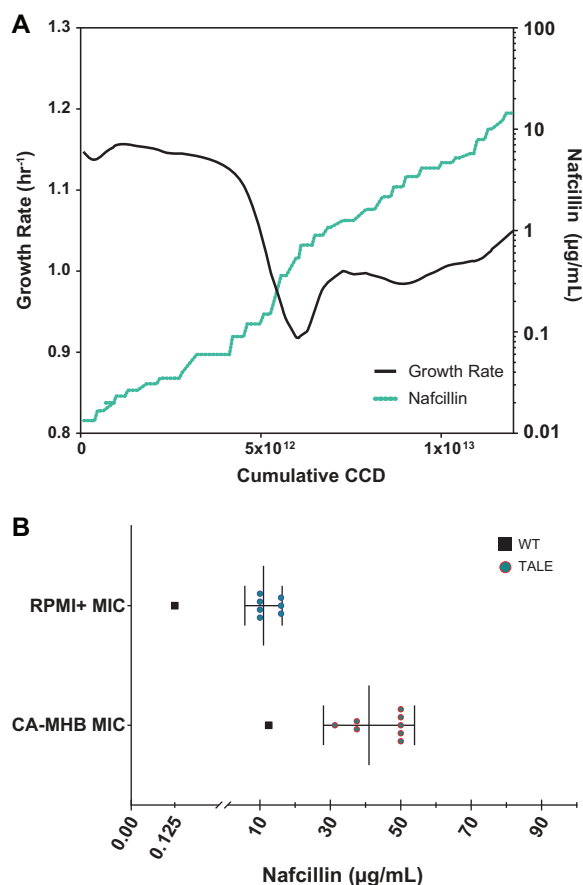


FIG 2 Nafcillin adaptation of medium-adapted strains derived from *S. aureus* TCH1516. (A) Fitness trajectory for a typical TALE experiment, showing population growth rate and continuously increasing antibiotic concentration. The selected trajectory depicts SNFR9 exposed to nafcillin in RPMI+. (B) A plot of the MICs for selected clones from endpoint populations after nafcillin tolerization. The MICs for the wild-type TCH1516 (black squares) and TALE strains (green circles) on the respective medium are shown.

medium adaptation ALEs (i.e., if the gene or genetic region contained multiple unique mutations or the same mutation across independent ALE replicates). On average, there were fewer mutations in response to nafcillin stress on CA-MHB compared to RPMI+, as represented by the key mutations in the endpoint clones and populations (Tables 3 and 4). Endpoint clones and populations from evolution experiments on CA-MHB led to the identification of 13 unique key mutations across 5 genes, while the ones performed on RPMI+ presented 25 unique key mutations across 10 genes (Tables 3 and 4).

In CA-MHB, the majority of key mutations had been previously identified as being related to a resistance phenotype. One of the most frequently mutated gene sets were those that encoded the regulatory system VraSRT. In fact, *vraT* is a negative regulator of the *vraSR* operon which controls transcription of a number of genetic determinants involved in cell wall synthesis and cell division (45). Five of the 13 total key mutations under this condition were SNPs in the genes of this system. This regulatory system has also been shown to be mutated under vancomycin selection pressure in a different USA300 *S. aureus* strain, which also decreased daptomycin susceptibility (46). Another mutated gene was *apt*, which also occurred in RPMI+ medium adaptation ALE. This is interesting, as this might be the reason why SNFM clones presented an improved growth rate in RPMI+ conditions (Fig. 3A). As discussed earlier, *apt* enables nucleotide salvage reactions, a much more energetically favorable pathway than *de novo* nucleotide synthesis (47), and it has been implicated in the stringent response of bacteria to stressful conditions (32, 48). Mutations resulting in an amino acid substitution and a premature stop codon were discovered in *pbuG*, which encodes a guanine/xanthine

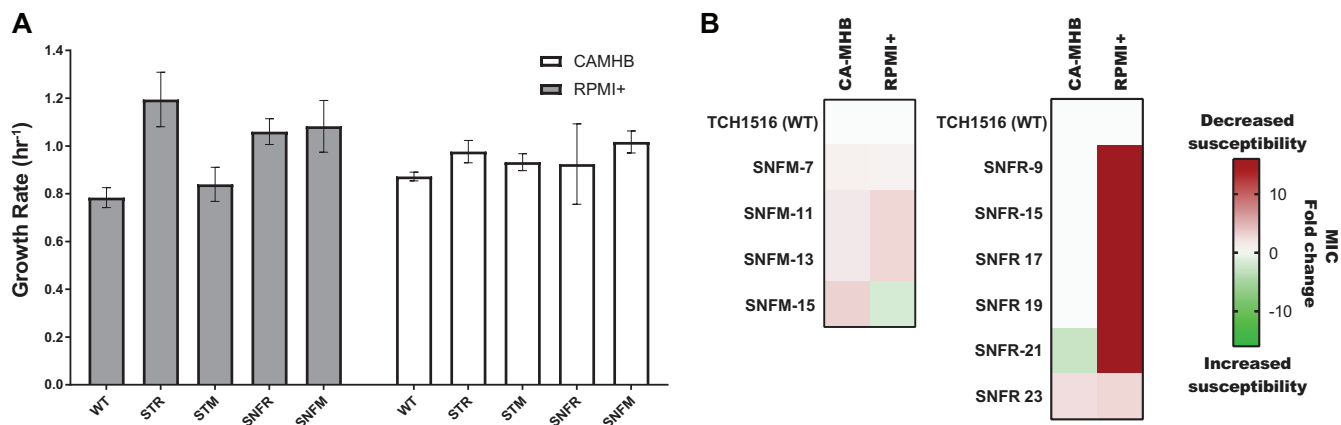


FIG 3 Phenotypic characterization of TALE strains. (A) Growth rates of wild-type, medium-adapted, and nafcillin-adapted strains. The graph shows the measured growth rates of several selected endpoint clones for strains derived from either RPMI+ (STR and SNFR) or CA-MHB (STM and SNFM) evolutionary conditions. White bars represent clonal growth rates in CA-MHB, and gray bars represent the growth rate for the same clones in RPMI+. The graph shows the growth rates of three tolerization endpoint clones from both medium conditions along a lineage. Data presented are averages from triplicates. A comprehensive ANOVA statistical analysis is provided in Table S5 in the supplemental material. (B) Heat map of the nafcillin MIC fold change of TALE strains compared to the wild-type MIC in both medium types. STM, *S. aureus* CA-MHB-adapted strain; STR, *S. aureus* RPMI+-adapted strain; SNFM, *S. aureus* nafcillin-adapted strain in CA-MHB; SNFR, *S. aureus* nafcillin-adapted strain in RPMI+.

permease. A *Bacillus subtilis* mutant with defects in *pbuG* displayed impaired uptake rates of nucleoside sugars guanine and hypoxanthine as well as resistance to toxic purine analog compounds (49). There has also been evidence to suggest a role between purine biosynthesis and increased resistance to vancomycin and daptomycin, two other membrane- and cell wall-targeting antibiotics (50, 51). The last key mutated gene that saw multiple mutations across TALE replicates in CA-MHB was *mgt*, or *sgtB* referred to elsewhere, whose gene product is a monofunctional glycosyltransferase responsible for elongation of the glycan strands using lipid-linked disaccharide-pentapeptide as the substrate (52). Each of the mutations in *sgtB* seems to lead to open reading frame disruption (Table 3), possibly abolishing its transcription. This glycosyltransferase is nonessential in *S. aureus* (53–56), but it seems to be upregulated upon treatment with cell wall-targeting antibiotics, including oxacillin (57). Furthermore,

TABLE 3 Key mutations for final endpoint clones of *S. aureus* TCH1516 after tolerance adaptive laboratory evolution in CA-MHB to nafcillin (SNFM)

Gene ^a	Specific function	Mutation type	Protein and nucleotide change ^b	Strain
<i>apt</i>	Adenine phosphoribosyltransferase	SNP	G59D (GGC→GAC)	11
		SNP	I127N (ATT→AAT)	19
		SNP	K82E (AAA→GAA)	13
<i>pbuG</i>	Xanthine/guanine permease	SNP	Q6* (CAG→TAG)	7
		SNP	A84E (GCA→GAA)	23
<i>vraS</i>	Two-component sensor histidine kinase	SNP	G330D (GGT→GAT)	11
		SNP	T331I (ACA→ATA)	19
<i>vraT</i> (RS10230)	Transporter associated with VraSR	SNP	T8K (ACG→AAG)	13
		SNP	V199A (GTT→GCT)	23
		SNP	P126S (CCA→TCA)	19
<i>sgtB</i> (<i>mgt</i>)	Monofunctional transglycosylase	DEL	(T)7→6, coding (109/810 nt)	11
		SNP	Q215* (CAA→TAA)	15
		SNP	S121* (TCA→TAA)	13

^aThe gene nomenclature provided by prokka annotation, reflected in the mutation analysis, is shown in the parentheses.

^bAn asterisk indicates that a mutation led to a stop codon being formed.

TABLE 4 Key mutations for final endpoint clones of *S. aureus* TCH1516 after tolerance adaptive laboratory evolution in RPMI+ to nafcillin (SNFR)

Gene ^a	Specific function	Mutation	Protein and nucleotide change ^b	Strain(s)
<i>mecA</i>	Beta-lactam-inducible penicillin-binding protein	SNP	D586Y (GAT→TAT)	7, 9, 13, 15, 17, 23
		SNP	V488F (GTT→TTT)	19
<i>rpoD</i> (<i>sigA</i>)	DNA-directed RNA polymerase sigma subunit	SNP	A187T (GCA→ACA)	13
		SNP	A194V (GCA→GTA)	19
<i>gdpP</i>	Cyclic di-AMP phosphodiesterase	SNP	N182K (AAC→AAG)	9
		SNP	S222F (TCC→TTC)	23
<i>ywtF</i>	Putative transcriptional regulator	DEL	Coding (235/1218 nt)	7
		SNP	Y121* (TAC→TAG)	15
		SNP	D214N (GAC→AAC)	19
<i>codY</i>	CodY family transcriptional regulator	SNP	S204L (TCA→TTA)	9
		SNP	K205N (AAA→AAT)	15
<i>cdaA</i>	Cyclic di-AMP synthase	SNP	W76C (TGG→TGC)	7
		SNP	Q55H (CAG→CAT)	13
		SNP	A80S (GCT→TCT)	17
<i>ssaA2_4</i>	Staphylococcal secretory antigen	SNP	W70* (TGG→TAG)	9
		SNP	C45Y (TGT→TAT)	15
		SNP	G65V (GGC→GTC)	17
<i>oatA</i> (<i>oatA_2</i>)	O-Acetyltransferase	SNP	G451S (GGT→AGT)	7
		DEL	Coding (1239-1250/1812 nt)	9
		DEL	Coding (29/1812 nt)	13
		DEL	Coding (1327/1812 nt)	15
		SNP	E341* (GAA→TAA)	19
<i>vraS</i>	Sensor histidine kinase	SNP	G92V (GGC→GTC)	7
		SNP	V66L (GTA→CTA)	17, 19, 23
<i>RS08710</i>	Heme uptake protein Mmpl11	DEL	Coding (2065-2067/2280 nt)	7, 19

^aThe gene nomenclature provided by prokka annotation, reflected in the mutation analysis, is shown in the parentheses. The gene locus tag corresponds to USA300HOU_RSXXXXX.

^bAn asterisk indicates that a mutation led to a stop codon being formed.

inactivation of *sgtB* in the USA300 *S. aureus* LAC strain has demonstrated increased resistance to several cell wall antibiotics (58).

In RPMI+, although there was a higher number of mutations, there was also a higher degree of parallelism, with 36% of key mutations compared to 25.5% in CA-MHB. The most targeted gene for mutation upon exposure to nafcillin in RPMI+ was *mecA* (Table 4). Mutations in *mecA* occurred in seven independent lineages, with an SNP at position 586 changing an aspartic acid residue to a tyrosine residue, comprising six of these mutations. Penicillin binding protein 2a (PBP2a) is encoded by *mecA* and is responsible for catalyzing transpeptidation of peptidoglycan during cell wall synthesis. The binding protein has long been thought to play a vital role in resistance to β -lactamase-resistant semisynthetic β -lactams (nafcillin, oxacillin, methicillin, etc.) due to its lower affinity for these antibiotics (59, 60). Emergence of *S. aureus* strains containing *mecA* has been hypothesized to be due in part to horizontal gene transfer from closely related staphylococcal species leading to formation of MRSA precursors (61). It has been discovered that PBP2a is essential for *S. aureus* survival, although it is able to replace transpeptidation activity by other PBPs, it still requires interaction with the transglycosylase activity of PBP2a (62).

Another highly mutated gene was *oatA*, which encodes an O-acetyltransferase. Genetic changes included formation of a premature stop codon, in-frame deletion of 12 bp, and two single base pair deletions. OatA encodes the enzyme required for

O-acetylation of peptidoglycan by translocation of acetyl groups from a cytoplasmic source across the membrane (61). These results are consistent with previous data showing that exposure of MRSA to methicillin results not only in reduced peptidoglycan cross-linking but also in reduced peptidoglycan O-acetylation (63). O-acetylation is important for resisting autolysis activity from lysozymes (64) and has been shown to increase susceptibility to certain β -lactams (65). Reduction in O-acetylation has great implications for the host-pathogen relationship in *S. aureus* infections. Strains with mutations in O-acetyltransferase are more effectively killed by macrophages (66). Furthermore, *S. aureus oat* mutants have been shown to release more interleukin 1 β (IL-1 β) (66), a critical factor in rapid clearance of *S. aureus* bacteremia, as shown by the fact that patients with persistent bacteremia on antimicrobial therapy fail to mount a robust IL-1 β response (67, 68). In fact, beta-lactam therapy has been shown to elicit a more robust IL-1 β response compared to vancomycin therapy in patients with *S. aureus* bacteremia to potentially explain, at least in part, the more favorable clinical and microbiological data of beta-lactams over vancomycin (69). Coupled with previously cited phenotypic studies, our findings showing *oat* mutations induced by nafcillin selection pressure in physiological media on MRSA show direct evidence for a specific attenuation of virulence occurring at a genetic locus. These findings lend strong support of the role of nafcillin (and potentially other beta-lactams) as a potentially important adjunct therapy in MRSA bacteremia to enhance bacteremia clearance as previously reported (70).

Similar to what has been observed for the CA-MHB TALEs, the *vraSRT* system was also mutated, in this case mostly *vraS*, with a higher preference for amino acid position 66, where a valine was replaced by a leucine. As mentioned earlier, this operon controls transcription of a number of genetic determinants involved in cell wall synthesis and cell division (45).

Two genes involved in regulating levels of cyclic diadenosine monophosphate (c-di-AMP) inside the cell were also mutated: *gdpP*, encoding a phosphodiesterase, and *cdsA* (also known as *dacA*), which encodes an adenylate cyclase. Both DacA and GdpP are involved in nucleotide signaling pathways, while the former produces c-di-AMP, the latter degrades the cyclic dinucleotide molecule (71, 72). Studies suggest that SNP mutations in *dacA*, distinct from the ones presented here, affect methicillin resistance via nucleotide signaling by reducing c-di-AMP, resulting in faster growing, less resistant, and more virulent strains (73). On the other hand, SNP mutations in *gdpP* have been observed in *S. aureus* after repeated exposure to oxacillin concentrations of 200 \times MIC and insertional mutants revealed increased tolerance to both oxacillin and vancomycin, as well as altered phenotypic signatures (74, 75). Also, clinical isolates from patients with *S. aureus* lacking *mecA* determinants were shown to have mutations in *gdpP*, further implicating the phosphodiesterase in resistance to β -lactams (76). Other mutations included the following: *ywtF*, encoding a putative transcriptional regulator, belonging to a family of regulators associated with influencing virulence factors, antibiotic resistance, and cell envelope maintenance in various *S. aureus* species (77–79); *codY*, encoding a transcriptional regulator that acts as a repressor for more than 100 genes associated with branched-chain amino acid metabolism and virulence production under nutrient limiting conditions (80–82); *rpoD*, encoding a RNA polymerase subunit; *ssaA2_4*, encoding a secretory antigen precursor; and *RS08710*, encoding a heme uptake-related protein.

The overlap between mutations conferring resistance to nafcillin on the genetic level in both medium types was minimal. The key mutation overlap between the two TALE medium conditions was reduced to the *vraSTR* operon. As previously mentioned, mutations within this operon have previously been shown to increase expression of a cell wall stress stimulon leading to thicker cell wall and envelope (45, 83). From all of the additional key mutations observed in CA-MHB nafcillin tolerized strains, *pbuG* and *sgtB* also occurred once in RPMI+ nafcillin tolerized strains, in one replicate each (Table S7). On the other hand, from the other key mutations observed in nafcillin RPMI+ tolerized strains, only the *oatA* gene was mutated once in one CA-MHB replicate

(Table S8). Interestingly, the genetic adaptation observed in the strains tolerized to nafcillin in RPMI+ did not translate to a resistant phenotype in CA-MHB (Fig. 3B), reiterating the medium-specific mechanisms employed toward nafcillin resistance. Nevertheless, the genes that were reproducibly mutated across the independent lineages under the CA-MHB and RPMI+ conditions have, for the most part, been previously identified as being associated with an antibiotic resistance phenotype.

DISCUSSION

For decades, methicillin-resistant *S. aureus* (MRSA) has been one of the major contributors to community- and hospital-acquired infections with a broad repertoire of infection type, severity, and human hosts (84). In the United States, this common commensal pathogen is responsible for more than 1 million cases of blood infection and close to 200,000 deaths (85). With such alarming figures, it becomes imperative to understand the underlying mechanisms of antibiotic resistance and adaptation to the host environment. Here, we present a method for determining differential mechanisms of resistance on the genetic level under different medium environments utilizing adaptive laboratory evolution, whole-genome sequencing, and phenotypic characterizations of evolved strains. Genotypes of generated strains were characterized to study fundamental underlying differences in how environmental considerations affect susceptibility at a systems level. Insights gained by analyzing repeatedly mutated regions across different medium conditions in tandem with phenotypic assessment can be leveraged to inform more effective treatment strategies and identify novel drug targets. Thus, the major findings from this work include the following: (i) a significant growth rate increase via genetic adaptation to physiological medium (RPMI+) compared to a negligible one observed in CAMHB; (ii) no gross virulence attenuation observed in medium-adapted strains in a pneumonia model of infection; (iii) medium-specific adaptation toward nafcillin tolerance, attributed to parallelly mutated genes, mostly related to membrane and cell wall integrity; (iv) key mutated genes previously shown to be associated with clinical resistant strains; (v) mutations in genetic loci under nafcillin selection pressure that could allow for enhanced intracellular survival. These findings support this approach to better understand clinically relevant adaptive strategies of bacteria that may influence not just antibiotic resistance, but also host-pathogen interactions.

Adaptive laboratory evolution was successful in generating medium-adapted strains of *S. aureus* TCH1516 to a more physiologically relevant medium, RPMI+. Strains adapted to RPMI+ (STR) saw an increase in growth rate, while no such increase was observed in CA-MHB-adapted strains (STM) (Fig. 1B). Mutations identified in RPMI+-adapted strains showed a high degree of evolutionary parallelism with mutations in the *apt* and *mntA* genes occurring in almost all of the independent ALE replicates (Table 1). Both gene products have been associated with the SOS stringent response in stressful conditions, while *mntA* specifically plays a key role in metal acquisition infection when the host limits availability (32, 39, 48, 86). A recent transcriptome analysis has shown that *S. aureus* TCH1516 is under manganese starvation upon cultivation in RPMI+ (96), strengthening the argument of a transcription and translation optimization of the *mnt* operon in the RPMI+ medium-adapted strains. Interestingly, mutations in *apt*, which enables nucleotide salvage reactions, were also identified in tolerance evolution to nafcillin, particularly when evolved on CA-MHB (Table 3). Mutations identified in this phosphoribosyltransferase likely play a crucial role in the improved growth rate in RPMI+ in the presence of no antibiotic for medium- and nafcillin-adapted strains (Fig. 3A).

The tolerance adaptive laboratory evolution (TALE) method proved successful in the generation of *S. aureus* TCH1516 strains resistant to nafcillin 2.5- to 4-fold higher compared to the wild type in CA-MHB and 80- to 160-fold higher in RPMI+ (Table 2 and Fig. 2B) after continuous exponential growth in the presence of increasing concentrations of nafcillin. The overlap of shared mutations between nafcillin resistance in each medium type point to several previously studied targets for antibiotic resistance (45, 54,

83). Evolution of antibiotic resistance in the tissue culture medium RPMI supplemented with 10% LB appears to enrich for several other mutations, particularly in *mecA* and other non-*mecA* genetic determinants (e.g., *oatA* and *vraS*). Mutations in *mecA* were all located in the active site of PBP2a (87), suggesting an alteration in the target for nafcillin, and thus enabling transpeptidase activity to proceed. Mutations affecting synthesis and acquisition of branched-chain amino acids, as well as biosynthesis of peptidoglycan and its precursors potentially suggest a reorganization of metabolic activity more representative of host infection (71, 81, 88). Importantly, mutations in *oatA* have been previously shown to have significant impact on *S. aureus* interaction with the host, potentially allowing enhanced intracellular survival to escape from largely extracellularly acting antibiotics like beta-lactams.

In summary, this study describes several mutations involved in adaptation to medium and nafcillin and discusses their possible role in those processes. These hypotheses warrant further investigation into the molecular mechanisms involved in such genetic adaptations, via reintroduction of such mutations into a wild-type strain using targeted genetic engineering approaches (89, 90) or biochemistry elucidation of protein activities and interactions. This study outlines specific mutations that can be tested via these approaches and provides strong contextual evidence of their causality. Furthermore, with a strain-agnostic approach, one could understand if these mutations are strain-specific or general adaptation mechanisms employed by *S. aureus* (91).

MATERIALS AND METHODS

Adaptive laboratory evolution and tolerance evolution of *S. aureus* USA300_TCH1516. The adaptive laboratory evolution (ALE) experiment was begun by streaking the wild-type *S. aureus* USA300_TCH1516 (taxid 451516) on LB agar plates. Colonies (five for CA-MHB and eight for RPMI+) were then selected and grown overnight at 37°C in the appropriate medium. Each individual flask served as the starting point for independent ALE experiments. An automated liquid handling platform (92) was used to serially propagate the growing cultures and monitor growth rates. Each batch culture was grown in 15 ml of the respective medium at 37°C and well aerated with magnetic stirrers at 1,800 rpm. When the optical density (OD) reached a value of 0.3, 150 μ l was inoculated into the next flask, thus maintaining a continuous exponential growth. The automated system measured the OD at 600 nm (OD₆₀₀) algorithmically on a Tecan Sunrise Absorbance Microplate reader. When the optical density reached a value of 0.3 (Tecan Sunrise plate reader equivalent to an OD₆₀₀ of 1 on a traditional spectrophotometer with a 1-cm path length), 150 μ l was inoculated into the next flask, thus maintaining a continuous exponential growth. The OD₆₀₀ values were converted to cell dry weight (DW) concentrations using a previously determined OD₆₀₀-dry cell weight relationship for *S. aureus* (1.0 OD₆₀₀ = 0.434 g DW/liter). Last, frozen stocks were taken intermittently throughout the course of the evolution experiments in 50% (vol/vol) glycerol solution and stored at -80°C. Tolerance evolution was performed similarly to medium adaptation as described above with the addition of continuously increasing concentration of nafcillin. The TALE method was adapted from the method in reference 93.

Growth rate calculations were determined and filtered if R^2 correlation was less than 0.98. Growth data were then smoothed to minimize noise following methods described in reference 94, by applying a three-median repeat smooth followed by convolution with a symmetrical kernel containing weights (1/4, 1/2, 1/4) and ended with final three-median smooth. Smoothed data were then fit to a piecewise cubic spline. The time scale of cumulative cell cycle divisions (CCD) was computed following methods outlined in reference 25.

MIC determination. Azithromycin (Fresenius Kabi), ceftazidime (Hospira), clindamycin (Pfizer), colistin (Xellia Pharmaceuticals ApS), daptomycin (Cubist Pharmaceuticals), linezolid (Pfizer), meropenem (Fresenius Kabi), and vancomycin (Mylan International) were purchased from a clinical pharmacy. Ampicillin, ciprofloxacin, gentamicin, and nafcillin were all purchased from Sigma-Aldrich. All drugs were resuspended in 1 × Dulbecco's phosphate-buffered saline (DPBS) (Corning).

The bacterial strains to be used in antibiotic susceptibility testing were first streaked on Luria agar plates from stocks stored at -80°C (in 20% glycerol and 80% Mueller-Hinton broth [MHB]) and grown stationary at 37°C overnight. Isolated colonies were picked from the plate and inoculated into 5 ml of either CA-MHB (MHB [Difco] amended with 20 mg/liter Ca²⁺ and 10 mg/liter Mg²⁺) or RPMI+ (phenol-free RPMI 1640 [Gibco] amended with 10% Luria-Delbruck [LB] [Criterion]) medium in a 14-ml Falcon polypropylene round-bottom snap cap tube (catalog no. 352059; Corning) and grown shaking at 100 rpm at 37°C overnight. The following day the overnight cultures were subcultured 1:50 in the desired medium and volume in either the 14-ml snap cap tubes and grown shaking at 100 rpm at 37°C until they reached mid-logarithmic phase (~OD₆₀₀ of 0.4). Unless otherwise noted, experiments were conducted in Costar flat-bottom 96 well plates (catalog no. 3370; Corning) with a final volume of 200 μ l/well.

For the MIC experiments, the bacteria were cultured in the same medium throughout (CA-MHB or RPMI+) prior to the addition of antibiotics. The mid-logarithmic-phase cultures were diluted to approximately 5×10^5 CFU (~OD₆₀₀ of 0.002), and 180 μ l was added to each experimental well of the 96-well

flat-bottom plate (catalog no. 3370; Costar). Either 20 μ l of 1 \times DPBS or 20 μ l of the desired 10 \times drug stock was added into each culture-containing well. The plates were then incubated shaking at 100 rpm at 37°C overnight. Bacterial growth, as determined by measuring the OD₆₀₀ of each well, was determined by utilizing an Enspire Alpha multimode plate reader (PerkinElmer). To determine the MIC₉₀, defined as the amount of drug required to inhibit \geq 90% of the growth of the untreated controls, the density of each drug-treated well was compared to the density of the untreated control well.

Mouse studies. All animal experiments were conducted under veterinary supervision and approved by the University of California San Diego (UCSD) IACUC. Bacterial pneumonia was established as previously described (29). In brief, *S. aureus* strains were grown overnight in cation-adjusted Mueller-Hinton broth (CA-MHB) and then used to inoculate fresh CA-MHB the day of the infection. Cultures were grown to logarithmic phase (\sim OD₆₀₀ of 0.4), washed three times in 1 \times DPBS (Corning), and resuspended to a concentration of 2.5 \times 10⁹ CFU/ml. Juvenile 8-week-old female C57Blk/6J mice were treated with 100 mg of ketamine (Koetis)/kg of body weight and 10 mg of xylazine (VetOne)/kg and then intratracheally infected with 40 μ l of the infection culture to give each mouse a 1 \times 10⁸ dose using an operating otoscope (Welch Allyn). Mice were allowed to recover on a sloped heating pad and then returned to their home cage. Mice were euthanized 24 h postinfection through CO₂ exposure followed by cervical dislocation. All five lobes of the lung were removed, placed into a 2-ml sterile microtube (Sarstedt) with 1 ml of 1 \times DPBS and 1-mm silica beads (Biospec), and homogenized for three cycles with one cycle consisting of 1 min on a MagNA lyser (Roche) followed by 1 min on ice. Homogenized samples were then serially diluted and spot plated on Luria agar (Criterion) plates, and then grown overnight at 37°C for CFU enumeration.

Whole-genome sequencing and identification of mutations. A total of 162 samples, including population and clonal samples were submitted for sequencing. Genomic DNA was isolated using Nucleospin Tissue kit (Macherey-Nagel). The resequencing library was constructed from the isolated genomic DNA using Kapa HyperPlus kit (Roche) according to the manufacturer's instructions. Then, the library was sequenced using a MiSeq reagent kit v3 (Illumina) in 600-cycle paired-end recipe on an MiSeq instrument (Illumina). Resequenced samples were then processed utilizing a modified script of the software breseq v.0.32.1 (30, 31) to map the genomes of the generated strains to the ancestral genome for identification of genetic mutations. All generated strains were mapped to *S. aureus* USA300_TCH1516 and reannotated using Prokka (95) (NCBI accession number GCA_000017085.1).

Data availability. Newly determined sequence data were deposited in the NCBI database under accession numbers [SRX3480972](https://ncbi.nlm.nih.gov/sra/SRX3480972) to [SRX3480983](https://ncbi.nlm.nih.gov/sra/SRX3480983) (STM), [SRR10341521](https://ncbi.nlm.nih.gov/sra/SRR10341521) to [SRR10341525](https://ncbi.nlm.nih.gov/sra/SRR10341525) (STM), [SRX3482887](https://ncbi.nlm.nih.gov/sra/SRX3482887) to [SRX3482918](https://ncbi.nlm.nih.gov/sra/SRX3482918) (STR), and [SRR8552775](https://ncbi.nlm.nih.gov/sra/SRR8552775) (SNFM and SNFR).

SUPPLEMENTAL MATERIAL

Supplemental material is available online only.

TEXT S1, DOCX file, 0.02 MB.

FIG S1, EPS file, 0.1 MB.

TABLE S1, DOCX file, 0.02 MB.

TABLE S2, DOCX file, 0.02 MB.

TABLE S3, XLSX file, 0.01 MB.

TABLE S4, XLSX file, 0.1 MB.

TABLE S5, DOCX file, 0.02 MB.

TABLE S6, DOCX file, 0.02 MB.

TABLE S7, XLSX file, 0.03 MB.

TABLE S8, XLSX file, 0.03 MB.

ACKNOWLEDGMENT

This research was supported by NIH NIAID grant (U01-AI124316).

We thank Patrick V. Phaneuf, Muyao Wu, Rodolfo A. Salido, Karenina Sanders, Caitriona Brennan, Gregory Humphrey, and Rob Knight for their assistance with whole genome sequencing and analysis.

REFERENCES

1. Tong SYC, Davis JS, Eichenberger E, Holland TL, Fowler VG, Jr. 2015. *Staphylococcus aureus* infections: epidemiology, pathophysiology, clinical manifestations, and management. *Clin Microbiol Rev* 28:603–661. <https://doi.org/10.1128/CMR.00134-14>.
2. Jevons MP. 1961. "Celbenin" - resistant *Staphylococci*. *BMJ* 1:124–125. <https://doi.org/10.1136/bmj.1.5219.124-a>.
3. Planet PJ, Diaz L, Kolokotronis S-O, Narechania A, Reyes J, Xing G, Rincon S, Smith H, Panesso D, Ryan C, Smith DP, Guzman M, Zurita J, Sebra R, Deikus G, Nolan RL, Tenover FC, Weinstock GM, Robinson DA, Arias CA. 2015. Parallel epidemics of community-associated methicillin-resistant *Staphylococcus aureus* USA300 infection in North and South America. *J Infect Dis* 212:1874–1882. <https://doi.org/10.1093/infdis/jiv320>.
4. Gonzalez BE, Martinez-Aguilar G, Hulten KG, Hammerman WA, Coss-Bu J, Avalos-Mishaan A, Mason EO, Jr, Kaplan SL. 2005. Severe staphylococcal sepsis in adolescents in the era of community-acquired methicillin-resistant *Staphylococcus aureus*. *Pediatrics* 115:642–648. <https://doi.org/10.1542/peds.2004-2300>.
5. World Health Organization. 1961. Standardization of methods for conducting microbic sensitivity tests: second report of the Expert Commit-

- tee on Antibiotics. World Health Organization Technical Report Series 210. World Health Organization, Geneva, Switzerland.
6. Hughes D, Andersson DI. 2017. Environmental and genetic modulation of the phenotypic expression of antibiotic resistance. *FEMS Microbiol Rev* 41:374–391. <https://doi.org/10.1093/femsre/fux004>.
 7. Kubicek-Sutherland JZ, Heithoff DM, Ersoy SC, Shimp WR, House JK, Marth JD, Smith JW, Mahan MJ. 2015. Host-dependent induction of transient antibiotic resistance: a prelude to treatment failure. *EBioMedicine* 2:1169–1178. <https://doi.org/10.1016/j.ebiom.2015.08.012>.
 8. Girardello R, Bispo PJM, Yamanaka TM, Gales AC. 2012. Cation concentration variability of four distinct Mueller-Hinton agar brands influences polymyxin B susceptibility results. *J Clin Microbiol* 50:2414–2418. <https://doi.org/10.1128/JCM.06686-11>.
 9. Barry AL, Reller LB, Miller GH, Washington JA, Schoenknecht FD, Peterson LR, Hare RS, Knapp C. 1992. Revision of standards for adjusting the cation content of Mueller-Hinton broth for testing susceptibility of *Pseudomonas aeruginosa* to aminoglycosides. *J Clin Microbiol* 30:585–589. [1551973] <https://doi.org/10.1128/JCM.30.3.585-589.1992>.
 10. Ersoy SC, Heithoff DM, Barnes L, V, Tripp GK, House JK, Marth JD, Smith JW, Mahan MJ. 2017. Correcting a fundamental flaw in the paradigm for antimicrobial susceptibility testing. *EBioMedicine* 20:173–181. <https://doi.org/10.1016/j.ebiom.2017.05.026>.
 11. Sakoulas G, Okumura CY, Thienphrapa W, Olson J, Nonejuie P, Dam Q, Dhand A, Pogliano J, Yeaman MR, Hensler ME, Bayer AS, Nizet V. 2014. Nafcillin enhances innate immune-mediated killing of methicillin-resistant *Staphylococcus aureus*. *J Mol Med (Berl)* 92:139–149. <https://doi.org/10.1007/s00109-013-1100-7>.
 12. Lin L, Nonejuie P, Munguia J, Hollands A, Olson J, Dam Q, Kumaraswamy M, Rivera H, Jr, Corriden R, Rohde M, Hensler ME, Burkart MD, Pogliano J, Sakoulas G, Nizet V. 2015. Azithromycin synergizes with cationic antimicrobial peptides to exert bactericidal and therapeutic activity against highly multidrug-resistant Gram-negative bacterial pathogens. *EBioMedicine* 2:690–698. <https://doi.org/10.1016/j.ebiom.2015.05.021>.
 13. Sandberg TE, Pedersen M, LaCroix RA, Ebrahim A, Bonde M, Herrgard MJ, Palsson BO, Sommer M, Feist AM. 2014. Evolution of *Escherichia coli* to 42°C and subsequent genetic engineering reveals adaptive mechanisms and novel mutations. *Mol Biol Evol* 31:2647–2662. <https://doi.org/10.1093/molbev/msu209>.
 14. Deatherage DE, Kepner JL, Bennett AF, Lenski RE, Barrick JE. 2017. Specificity of genome evolution in experimental populations of *Escherichia coli* evolved at different temperatures. *Proc Natl Acad Sci U S A* 114:E1904–E1912. <https://doi.org/10.1073/pnas.1616132114>.
 15. Toprak E, Veres A, Michel J-B, Chait R, Hartl DL, Kishony R. 2011. Evolutionary paths to antibiotic resistance under dynamically sustained drug selection. *Nat Genet* 44:101–105.
 16. Jahn LJ, Munck C, Ellabaan MMH, Sommer M. 2017. Adaptive laboratory evolution of antibiotic resistance using different selection regimes lead to similar phenotypes and genotypes. *Front Microbiol* 8:816. <https://doi.org/10.3389/fmicb.2017.00816>.
 17. Baym M, Lieberman TD, Kelsic ED, Chait R, Gross R, Yelin I, Kishony R. 2016. Spatiotemporal microbial evolution on antibiotic landscapes. *Science* 353:1147–1151. <https://doi.org/10.1126/science.aag0822>.
 18. Hattangady DS, Singh AK, Muthaiyan A, Jayaswal RK, Gustafson JE, Ulanov AV, Li Z, Wilkinson BJ, Pfeltz RF. 2015. Genomic, transcriptomic and metabolomic studies of two well-characterized, laboratory-derived vancomycin-intermediate *Staphylococcus aureus* strains derived from the same parent strain. *Antibiotics (Basel)* 4:76–112. <https://doi.org/10.3390/antibiotics4010076>.
 19. Friedman L, Alder JD, Silverman JA. 2006. Genetic changes that correlate with reduced susceptibility to daptomycin in *Staphylococcus aureus*. *Antimicrob Agents Chemother* 50:2137–2145. <https://doi.org/10.1128/AAC.00039-06>.
 20. Raafat D, Leib N, Wilmes M, François P, Schrenzel J, Sahl H-G. 2017. Development of in vitro resistance to chitosan is related to changes in cell envelope structure of *Staphylococcus aureus*. *Carbohydr Polym* 157:146–155. <https://doi.org/10.1016/j.carbpol.2016.09.075>.
 21. Ling LL, Schneider T, Peoples AJ, Spoering AL, Engels I, Conlon BP, Mueller A, Schäberle TF, Hughes DE, Epstein S, Jones M, Lazarides L, Steadman VA, Cohen DR, Felix CR, Fetterman KA, Millett WP, Nitti AG, Zullo AM, Chen C, Lewis K. 2015. A new antibiotic kills pathogens without detectable resistance. *Nature* 517:455–459. <https://doi.org/10.1038/nature14098>.
 22. Klein K, Grønne RB, Alm M, Brinch KS, Kolmos HJ, Andersen TE. 2017. Controlled release of plectasin N22114 from a hybrid silicone-hydrogel material for inhibition of *Staphylococcus aureus* biofilm. *Antimicrob Agents Chemother* 61:e00604-17. <https://doi.org/10.1128/AAC.00604-17>.
 23. Bonow RO, Carabello BA, Chatterjee K, de Leon AC, Jr, Faxon DP, Freed MD, Gaasch WH, Lytle BW, Nishimura RA, O'Gara PT, O'Rourke RA, Otto CM, Shah PM, Shanewise JS, Smith SC, Jacobs AK, Adams CD, Anderson JL, Antman EM, Faxon DP, Fuster V, Halperin JL, Hiratzka LF, Hunt SA, Lytle BW, Nishimura R, Page RL, Riegel B. 2006. ACC/AHA 2006 guidelines for the management of patients with valvular heart disease: a report of the American College of Cardiology/American Heart Association Task Force on Practice Guidelines (writing committee to revise the 1998 Guidelines for the Management of Patients With Valvular Heart Disease): developed in collaboration with the Society of Cardiovascular Anesthesiologists: endorsed by the Society for Cardiovascular Angiography and Interventions and the Society of Thoracic Surgeons. *Circulation* 114:e84–e231.
 24. Bennett JE, Dolin R, Blaser MJ. 2014. Principles and practice of infectious diseases. Elsevier Saunders, Philadelphia, PA.
 25. Lee D-H, Feist AM, Barrett CL, Palsson BØ. 2011. Cumulative number of cell divisions as a meaningful timescale for adaptive laboratory evolution of *Escherichia coli*. *PLoS One* 6:e26172. <https://doi.org/10.1371/journal.pone.0026172>.
 26. Rodriguez de Evgrafov M, Gumpert H, Munck C, Thomsen TT, Sommer MOA. 2015. Collateral resistance and sensitivity modulate evolution of high-level resistance to drug combination treatment in *Staphylococcus aureus*. *Mol Biol Evol* 32:1175–1185. <https://doi.org/10.1093/molbev/msv006>.
 27. Kubicek-Sutherland JZ, Lofton H, Vestergaard M, Hjort K, Ingmer H, Andersson DI. 2017. Antimicrobial peptide exposure selects for *Staphylococcus aureus* resistance to human defence peptides. *J Antimicrob Chemother* 72:115–127. <https://doi.org/10.1093/jac/dkw381>.
 28. Fux CA, Shirliff M, Stoodley P, Costerton JW. 2005. Can laboratory reference strains mirror "real-world" pathogenesis? *Trends Microbiol* 13:58–63. <https://doi.org/10.1016/j.tim.2004.11.001>.
 29. Dillon N, Holland M, Tsunemoto H, Hancock B, Cornax I, Pogliano J, Sakoulas G, Nizet V. 2019. Surprising synergy of dual translation inhibition vs. *Acinetobacter baumannii* and other multidrug-resistant bacterial pathogens. *EBioMedicine* 46:193–201. <https://doi.org/10.1016/j.ebiom.2019.07.041>.
 30. Deatherage DE, Barrick JE. 2014. Identification of mutations in laboratory-evolved microbes from next-generation sequencing data using breseq. *Methods Mol Biol* 1151:165–188. https://doi.org/10.1007/978-1-4939-0554-6_12.
 31. Phaneuf PV, Gosting D, Palsson B, Feist A. 2018. ALEdb 1.0: a database of mutations from adaptive laboratory evolution. *bioRxiv* <https://doi.org/10.1101/320747>.
 32. Huang Y-J, Tsai T-Y, Pan T-M. 2007. Physiological response and protein expression under acid stress of *Escherichia coli* O157:H7 TW01 isolated from Taiwan. *J Agric Food Chem* 55:7182–7191. <https://doi.org/10.1021/jf071014s>.
 33. Mann EE, Rice KC, Boles BR, Endres JL, Ranjit D, Chandramohan L, Tsang LH, Smeltzer MS, Horswill AR, Bayles KW. 2009. Modulation of eDNA release and degradation affects *Staphylococcus aureus* biofilm maturation. *PLoS One* 4:e5822. <https://doi.org/10.1371/journal.pone.0005822>.
 34. Okshevsky M, Meyer RL. 2015. The role of extracellular DNA in the establishment, maintenance and perpetuation of bacterial biofilms. *Crit Rev Microbiol* 41:341–352. <https://doi.org/10.3109/1040841X.2013.841639>.
 35. DeFrancesco AS, Masloboeva N, Syed AK, DeLoughery A, Bradshaw N, Li G-W, Gilmore MS, Walker S, Losick R. 2017. Genome-wide screen for genes involved in eDNA release during biofilm formation by *Staphylococcus aureus*. *Proc Natl Acad Sci U S A* 114:E5969–E5978. <https://doi.org/10.1073/pnas.1704544114>.
 36. Horsburgh MJ, Wharton SJ, Cox AG, Ingham E, Peacock S, Foster SJ. 2002. MntR modulates expression of the PerR regulon and superoxide resistance in *Staphylococcus aureus* through control of manganese uptake. *Mol Microbiol* 44:1269–1286. <https://doi.org/10.1046/j.1365-2958.2002.02944.x>.
 37. Hecht A, Glasgow J, Jaschke PR, Bawazer LA, Munson MS, Cochran JR, Endy D, Salit M. 2017. Measurements of translation initiation from all 64 codons in *E. coli*. *Nucleic Acids Res* 45:3615–3626. <https://doi.org/10.1093/nar/gkx070>.
 38. Belinky F, Rogozin IB, Koonin EV. 2017. Selection on start codons in prokaryotes and potential compensatory nucleotide substitutions. *Sci Rep* 7:12422. <https://doi.org/10.1038/s41598-017-12619-6>.

39. Hood MI, Skaar EP. 2012. Nutritional immunity: transition metals at the pathogen-host interface. *Nat Rev Microbiol* 10:525–537. <https://doi.org/10.1038/nrmicro2836>.
40. Diep BA, Phung Q, Date S, Arnott D, Bakalarski C, Xu M, Nakamura G, Swem DL, Alexander MK, Le HN, Mai TT, Tan M-W, Brown EJ, Nishiyama M. 2014. Identifying potential therapeutic targets of methicillin-resistant *Staphylococcus aureus* through in vivo proteomic analysis. *J Infect Dis* 209:1533–1541. <https://doi.org/10.1093/infdis/jit662>.
41. Cassat JE, Skaar EP. 2012. Metal ion acquisition in *Staphylococcus aureus*: overcoming nutritional immunity. *Semin Immunopathol* 34:215–235. <https://doi.org/10.1007/s00281-011-0294-4>.
42. Juttukonda LJ, Berends ETM, Zackular JP, Moore JL, Stier MT, Zhang Y, Schmitz JE, Beavers WN, Wijers CD, Gilston BA, Kehl-Fie TE, Atkinson J, Washington MK, Peebles RS, Chazin WJ, Torres VJ, Caprioli RM, Skaar EP. 2017. Dietary manganese promotes staphylococcal infection of the heart. *Cell Host Microbe* 22:531–542.e8. <https://doi.org/10.1016/j.chom.2017.08.009>.
43. Lee HH, Molla MN, Cantor CR, Collins JJ. 2010. Bacterial charity work leads to population-wide resistance. *Nature* 467:82–85. <https://doi.org/10.1038/nature09354>.
44. Yurtsev EA, Chao HX, Datta MS, Artemova T, Gore J. 2013. Bacterial cheating drives the population dynamics of cooperative antibiotic resistance plasmids. *Mol Syst Biol* 9:683. <https://doi.org/10.1038/msb.2013.39>.
45. Boyle-Vavra S, Yin S, Jo DS, Montgomery CP, Daum RS. 2013. VraT/YvqF is required for methicillin resistance and activation of the VraSR regulon in *Staphylococcus aureus*. *Antimicrob Agents Chemother* 57:83–95. <https://doi.org/10.1128/AAC.01651-12>.
46. Passalacqua KD, Satola SW, Crispell EK, Read TD. 2012. A mutation in the PP2C phosphatase gene in a *Staphylococcus aureus* USA300 clinical isolate with reduced susceptibility to vancomycin and daptomycin. *Antimicrob Agents Chemother* 56:5212–5223. <https://doi.org/10.1128/AAC.05770-11>.
47. Moffatt BA, Ashihara H. 2002. Purine and pyrimidine nucleotide synthesis and metabolism. *Arabidopsis Book* 1:e0018. <https://doi.org/10.1199/tab.0018>.
48. Anderson KL, Roux CM, Olson MW, Luong TT, Lee CY, Olson R, Dunman PM. 2010. Characterizing the effects of inorganic acid and alkaline shock on the *Staphylococcus aureus* transcriptome and messenger RNA turnover. *FEMS Immunol Med Microbiol* 60:208–250. <https://doi.org/10.1111/j.1574-695X.2010.00736.x>.
49. Saxild HH, Nygaard P. 1987. Genetic and physiological characterization of *Bacillus subtilis* mutants resistant to purine analogs. *J Bacteriol* 169:2977–2983. [3110131] <https://doi.org/10.1128/JB.169.7.2977-2983.1987>.
50. Mongodin E, Finan J, Climo MW, Rosato A, Gill S, Archer GL. 2003. Microarray transcription analysis of clinical *Staphylococcus aureus* isolates resistant to vancomycin. *J Bacteriol* 185:4638–4643. <https://doi.org/10.1128/JB.185.15.4638-4643.2003>.
51. Gaupp R, Lei S, Reed JM, Peisker H, Boyle-Vavra S, Bayer AS, Bischoff M, Herrmann M, Daum RS, Powers R, Somerville GA. 2015. *Staphylococcus aureus* metabolic adaptations during the transition from a daptomycin susceptibility phenotype to a daptomycin nonsusceptibility phenotype. *Antimicrob Agents Chemother* 59:4226–4238. <https://doi.org/10.1128/AAC.00160-15>.
52. Wang QM, Peery RB, Johnson RB, Alborn WE, Yeh WK, Skatrud PL. 2001. Identification and characterization of a monofunctional glycosyltransferase from *Staphylococcus aureus*. *J Bacteriol* 183:4779–4785. <https://doi.org/10.1128/JB.183.16.4779-4785.2001>.
53. Reynolds PE, Brown DF. 1985. Penicillin-binding proteins of beta-lactam-resistant strains of *Staphylococcus aureus*. Effect of growth conditions. *FEBS Lett* 192:28–32. [3850810] [https://doi.org/10.1016/0014-5793\(85\)80036-3](https://doi.org/10.1016/0014-5793(85)80036-3).
54. Reed P, Atilano ML, Alves R, Hoiczky E, Sher X, Reichmann NT, Pereira PM, Roemer T, Filipe SR, Pereira-Leal JB, Ligoxygakis P, Pinho MG. 2015. *Staphylococcus aureus* survives with a minimal peptidoglycan synthesis machine but sacrifices virulence and antibiotic resistance. *PLoS Pathog* 11:e1004891. <https://doi.org/10.1371/journal.ppat.1004891>.
55. Rebets Y, Lupoli T, Qiao Y, Schirner K, Villet R, Hooper D, Kahne D, Walker S. 2014. Moenomycin resistance mutations in *Staphylococcus aureus* reduce peptidoglycan chain length and cause aberrant cell division. *ACS Chem Biol* 9:459–467. <https://doi.org/10.1021/cb4006744>.
56. Reed P, Veiga H, Jorge AM, Terrak M, Pinho MG. 2011. Monofunctional transglycosylases are not essential for *Staphylococcus aureus* cell wall synthesis. *J Bacteriol* 193:2549–2556. <https://doi.org/10.1128/JB.01474-10>.
57. Utaida S, Dunman PM, Macapagal D, Murphy E, Projan SJ, Singh VK, Jayaswal RK, Wilkinson BJ. 2003. Genome-wide transcriptional profiling of the response of *Staphylococcus aureus* to cell-wall-active antibiotics reveals a cell-wall-stress stimulon. *Microbiology* 149:2719–2732. <https://doi.org/10.1099/mic.0.26426-0>.
58. Karinou E, Pazos M, Vollmer W, Gründling A. 2018. Inactivation of the monofunctional peptidoglycan glycosyltransferase SgTB allows *Staphylococcus aureus* to survive in the absence of lipoteichoic acid. *bioRxiv* <https://doi.org/10.1101/311282>.
59. Hartman BJ, Tomasz A. 1984. Low-affinity penicillin-binding protein associated with beta-lactam resistance in *Staphylococcus aureus*. *J Bacteriol* 158:513–516. [6563036] <https://doi.org/10.1128/JB.158.2.513-516.1984>.
60. Utsui Y, Yokota T. 1985. Role of an altered penicillin-binding protein in methicillin- and cephem-resistant *Staphylococcus aureus*. *Antimicrob Agents Chemother* 28:397–403. [3878127] <https://doi.org/10.1128/AAC.28.3.397>.
61. Musser JM, Kapur V. 1992. Clonal analysis of methicillin-resistant *Staphylococcus aureus* strains from intercontinental sources: association of the mec gene with divergent phylogenetic lineages implies dissemination by horizontal transfer and recombination. *J Clin Microbiol* 30:2058–2063. [1500513] <https://doi.org/10.1128/JCM.30.8.2058-2063.1992>.
62. Pinho MG, de Lencastre H, Tomasz A. 2001. An acquired and a native penicillin-binding protein cooperate in building the cell wall of drug-resistant staphylococci. *Proc Natl Acad Sci U S A* 98:10886–10891. <https://doi.org/10.1073/pnas.191260798>.
63. Qoronfleh MW, Wilkinson BJ. 1986. Effects of growth of methicillin-resistant and -susceptible *Staphylococcus aureus* in the presence of beta-lactams on peptidoglycan structure and susceptibility to lytic enzymes. *Antimicrob Agents Chemother* 29:250–257. [2872855] <https://doi.org/10.1128/AAC.29.2.250>.
64. Pushkaran AC, Nataraj N, Nair N, Götz F, Biswas R, Mohan CG. 2015. Understanding the structure-function relationship of lysozyme resistance in *Staphylococcus aureus* by peptidoglycan O-acetylation using molecular docking, dynamics, and lysis assay. *J Chem Inf Model* 55:760–770. <https://doi.org/10.1021/ci500734k>.
65. Crisóstomo MI, Vollmer W, Kharat AS, Inhülsen S, Gehre F, Buckenmaier S, Tomasz A. 2006. Attenuation of penicillin resistance in a peptidoglycan O-acetyl transferase mutant of *Streptococcus pneumoniae*. *Mol Microbiol* 61:1497–1509. <https://doi.org/10.1111/j.1365-2958.2006.05340.x>.
66. Shimada T, Park BG, Wolf AJ, Brikos C, Goodridge HS, Becker CA, Reyes CN, Miao EA, Aderem A, Götz F, Liu GY, Underhill DM. 2010. *Staphylococcus aureus* evades lysozyme-based peptidoglycan digestion that links phagocytosis, inflammasome activation, and IL-1 β secretion. *Cell Host Microbe* 7:38–49. <https://doi.org/10.1016/j.chom.2009.12.008>.
67. Rose WE, Eickhoff JC, Shukla SK, Pantrangi M, Rooijackers S, Cosgrove SE, Nizet V, Sakoulas G. 2012. Elevated serum interleukin-10 at time of hospital admission is predictive of mortality in patients with *Staphylococcus aureus* bacteremia. *J Infect Dis* 206:1604–1611. <https://doi.org/10.1093/infdis/jis552>.
68. Rose WE, Shukla SK, Berti AD, Hayney MS, Henriquez KM, Ranzoni A, Cooper MA, Proctor RA, Nizet V, Sakoulas G. 2017. Increased endovascular *Staphylococcus aureus* inoculum is the link between elevated serum interleukin 10 concentrations and mortality in patients with bacteremia. *Clin Infect Dis* 64:1406–1412. <https://doi.org/10.1093/cid/cix157>.
69. Volk CF, Burgdorf S, Edwardson G, Nizet V, Sakoulas G, Rose WE. 1 August 2019. IL-1 β and IL-10 host responses in patients with *Staphylococcus aureus* bacteremia determined by antimicrobial therapy. *Clin Infect Dis* <https://doi.org/10.1093/cid/ciz686>.
70. Geriak M, Haddad F, Rizvi K, Rose W, Kullar R, LaPlante K, Yu M, Vasina L, Ouellette K, Zervos M, Nizet V, Sakoulas G. 2019. Clinical data on daptomycin plus ceftaroline versus standard of care monotherapy in the treatment of methicillin-resistant *Staphylococcus aureus* bacteremia. *Antimicrob Agents Chemother* 63:e02483-18.
71. Corrigan RM, Bowman L, Willis AR, Kaever V, Gründling A. 2015. Crosstalk between two nucleotide-signaling pathways in *Staphylococcus aureus*. *J Biol Chem* 290:5826–5839. <https://doi.org/10.1074/jbc.M114.598300>.
72. Corrigan RM, Abbott JC, Burhenne H, Kaever V, Gründling A. 2011. c-di-AMP is a new second messenger in *Staphylococcus aureus* with a role in controlling cell size and envelope stress. *PLoS Pathog* 7:e1002217. <https://doi.org/10.1371/journal.ppat.1002217>.
73. Dengler V, McCallum N, Kiefer P, Christen P, Patrignani A, Vorholt JA,

- Berger-Bächi B, Senn MM. 2013. Mutation in the c-di-AMP cyclase *dacA* affects fitness and resistance of methicillin resistant *Staphylococcus aureus*. *PLoS One* 8:e73512. <https://doi.org/10.1371/journal.pone.0073512>.
74. Griffiths JM, O'Neill AJ. 2012. Loss of function of the *gdpP* protein leads to joint β -lactam/glycopeptide tolerance in *Staphylococcus aureus*. *Antimicrob Agents Chemother* 56:579–581. <https://doi.org/10.1128/AAC.05148-11>.
75. Chung M, Borges V, Gomes JP, de Lencastre H, Tomasz A. 2018. Phenotypic signatures and genetic determinants of oxacillin tolerance in a laboratory mutant of *Staphylococcus aureus*. *PLoS One* 13:e0199707. <https://doi.org/10.1371/journal.pone.0199707>.
76. Argudín MA, Roisin S, Nienhaus L, Dodémond M, de Mendonça R, Nonhoff C, Deplano A, Denis O. 2018. Genetic diversity among *Staphylococcus aureus* isolates showing oxacillin and/or cefoxitin resistance not linked to the presence of *mec* genes. *Antimicrob Agents Chemother* 62:e00091-18. <https://doi.org/10.1128/AAC.00091-18>.
77. Hübscher J, Lüthy L, Berger-Bächi B, Stutzmann Meier P. 2008. Phylogenetic distribution and membrane topology of the LytR-CpsA-Psr protein family. *BMC Genomics* 9:617. <https://doi.org/10.1186/1471-2164-9-617>.
78. Chan YGY, Frankel MB, Dengler V, Schneewind O, Missiakas D. 2013. *Staphylococcus aureus* mutants lacking the LytR-CpsA-Psr (LCP) family of enzymes release wall teichoic acids into the extracellular medium. *J Bacteriol* 195:4650–4659. <https://doi.org/10.1128/JB.00544-13>.
79. Siegel SD, Liu J, Ton-That H. 2016. Biogenesis of the Gram-positive bacterial cell envelope. *Curr Opin Microbiol* 34:31–37. <https://doi.org/10.1016/j.mib.2016.07.015>.
80. Waters NR, Samuels DJ, Behera RK, Livny J, Rhee KY, Sadykov MR, Brinsmade SR. 2016. A spectrum of CodY activities drives metabolic reorganization and virulence gene expression in *Staphylococcus aureus*. *Mol Microbiol* 101:495–514. <https://doi.org/10.1111/mmi.13404>.
81. Kaiser JC, King AN, Grigg JC, Sheldon JR, Edgell DR, Murphy MEP, Brinsmade SR, Heinrichs DE. 2018. Repression of branched-chain amino acid synthesis in *Staphylococcus aureus* is mediated by isoleucine via CodY, and by a leucine-rich attenuator peptide. *PLoS Genet* 14:e1007159. <https://doi.org/10.1371/journal.pgen.1007159>.
82. Sonenshein AL. 2005. CodY, a global regulator of stationary phase and virulence in Gram-positive bacteria. *Curr Opin Microbiol* 8:203–207. <https://doi.org/10.1016/j.mib.2005.01.001>.
83. McCallum N, Meier PS, Heusser R, Berger-Bächi B. 2011. Mutational analyses of open reading frames within the *vraSR* operon and their roles in the cell wall stress response of *Staphylococcus aureus*. *Antimicrob Agents Chemother* 55:1391–1402. <https://doi.org/10.1128/AAC.01213-10>.
84. Kuroda M, Ohta T, Uchiyama I, Baba T, Yuzawa H, Kobayashi I, Cui L, Oguchi A, Aoki K, Nagai Y, Lian J, Ito T, Kanamori M, Matsumaru H, Maruyama A, Murakami H, Hosoyama A, Mizutani-Ui Y, Takahashi NK, Sawano T, Inoue R, Kaito C, Sekimizu K, Hirakawa H, Kuhara S, Goto S, Yabuzaki J, Kanehisa M, Yamashita A, Oshima K, Furuya K, Yoshino C, Shiba T, Hattori M, Ogasawara N, Hayashi H, Hiramatsu K. 2001. Whole genome sequencing of methicillin-resistant *Staphylococcus aureus*. *Lancet* 357:1225–1240. [https://doi.org/10.1016/S0140-6736\(00\)04403-2](https://doi.org/10.1016/S0140-6736(00)04403-2).
85. Angus DC, van der Poll T. 2013. Severe sepsis and septic shock. *N Engl J Med* 369:840–851. <https://doi.org/10.1056/NEJMra1208623>.
86. Kehl-Fie TE, Zhang Y, Moore JL, Farrand AJ, Hood MI, Rath S, Chazin WJ, Caprioli RM, Skaar EP. 2013. MntABC and MntH contribute to systemic *Staphylococcus aureus* infection by competing with calprotectin for nutrient manganese. *Infect Immun* 81:3395–3405. <https://doi.org/10.1128/IAI.00420-13>.
87. Lim D, Strynadka N. 2002. Structural basis for the beta lactam resistance of PBP2a from methicillin-resistant *Staphylococcus aureus*. *Nat Struct Biol* 9:870–876.
88. Sychantha D, Jones CS, Little DJ, Moynihan PJ, Robinson H, Galley NF, Roper DI, Dowson CG, Howell PL, Clarke AJ. 2017. In vitro characterization of the antiviral target of Gram-positive pathogens, peptidoglycan O-acetyltransferase A (OatA). *PLoS Pathog* 13:e1006667. <https://doi.org/10.1371/journal.ppat.1006667>.
89. Prax M, Lee CY, Bertram R. 2013. An update on the molecular genetics toolbox for staphylococci. *Microbiology* 159:421–435. <https://doi.org/10.1099/mic.0.061705-0>.
90. Penewit K, Holmes EA, McLean K, Ren M, Waalkes A, Salipante SJ. 2018. Efficient and scalable precision genome editing in *Staphylococcus aureus* through conditional recombineering and CRISPR/Cas9-mediated counterselection. *mBio* 9:e00067-18. <https://doi.org/10.1128/mBio.00067-18>.
91. Machado H, Weng LL, Dillon N, Seif Y, Holland M, Pekar JE, Monk JM, Nizet V, Palsson BO, Feist AM. 2019. Strain-specific metabolic requirements revealed by a defined minimal medium for systems analyses of *Staphylococcus aureus*. *Appl Environ Microbiol* 85:e01773-19. <https://doi.org/10.1128/AEM.01773-19>.
92. LaCroix RA, Palsson BO, Feist AM. 2017. A model for designing adaptive laboratory evolution experiments. *Appl Environ Microbiol* 83:e03115-16. <https://doi.org/10.1128/AEM.03115-16>.
93. Mohamed ET, Wang S, Lennen RM, Herrgård MJ, Simmons BA, Singer SW, Feist AM. 2017. Generation of a platform strain for ionic liquid tolerance using adaptive laboratory evolution. *Microb Cell Fact* 16:204. <https://doi.org/10.1186/s12934-017-0819-1>.
94. Beyer H. 1981. Tukey, John W.: *Exploratory Data Analysis*. Addison-Wesley Publishing Company Reading, Mass. — Menlo Park, Cal., London, Amsterdam, Don Mills, Ontario, Sydney 1977, XVI, 688 S. *Biom J* 23: 413–414. <https://doi.org/10.1002/bimj.4710230408>.
95. Seemann T. 2014. Prokka: rapid prokaryotic genome annotation. *Bioinformatics* 30:2068–2069. <https://doi.org/10.1093/bioinformatics/btu153>.
96. Poudel S, Tsunemoto H, Seif Y, Sastry AV, Szubin R, Xu S, Machado H, Olson C, Anand A, Pogliano J, Nizet V, Palsson B. 2020. Revealing 29 sets of independently modulated genes in *Staphylococcus aureus*, their regulators and role in key physiological responses. *bioRxiv* <https://doi.org/10.1101/2020.03.18.997296>.